CHAPTER 3

RESULTS AND DISCUSSION

3.1 Electrochemical behavior of metals

3.1.1 Cyclic voltammetry of blank solution at glassy carbon electrode

Cyclic voltammogram of CH_3CN containing 0.1 M TBAP as a supporting electrolyte as blank solutions were recorded in the potential window of -3.000 V to 3.000 V vs Ag/AgCl. No significant peak was obtained, indicating that there were no sinificant impurities as shown in Figure 3-1.

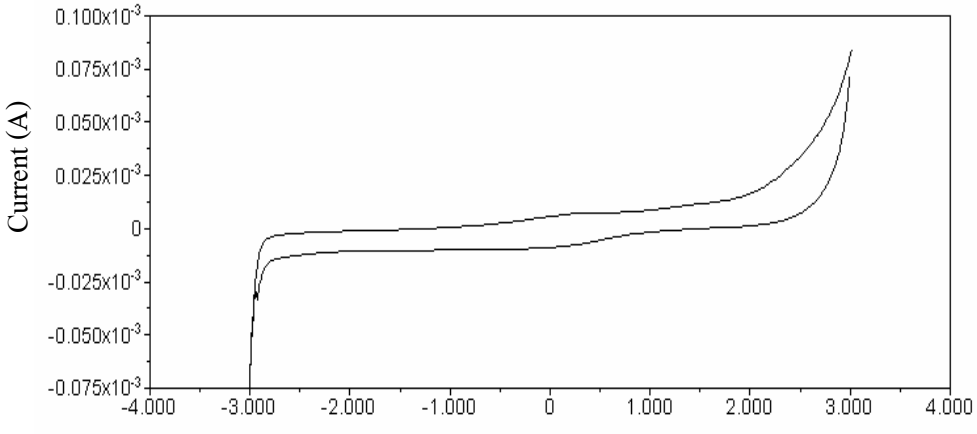

Figure 3-1 Cyclic voltammogram of blank solution at glassy carbon electrode in 50 mL CH_3CN containing 0.1 M TBAP with scan rate of 100 mV s^{-1}

3.1.2 Cyclic voltammetry of Pb(II) solution at glassy carbon electrode

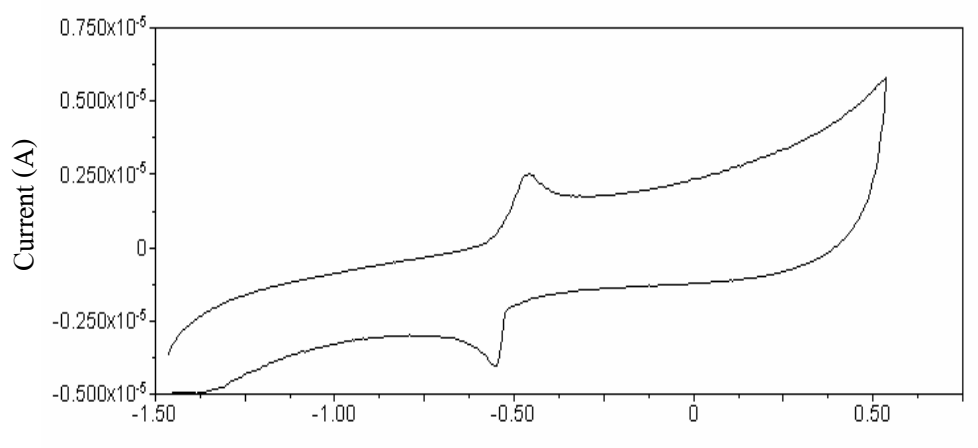

Figure 3-2 Cyclic voltammogram of 207.20 mg L^{-1} Pb(II) at glassy carbon electrode in 50 mL CH_3CN containing 0.1 M TBAP with scan rate of 100 mV s^{-1}

Cyclic voltammogram of 207.20 mg L^{-1} Pb(II) in CH_3CN containing 0.1 M TBAP as electrolyte is shown in Figure 3-2. The resting potential is 0.036 V. The reduction peak (Epc) appears at -0.548 V vs Ag/AgCl and Ipc = 1.985×10^{-6} A. When the scan is reversed, the oxidation peak (Epa) occurs at -0.460 V vs Ag/AgCl and Ipa = 1.740×10^{-6} A. The reduction reaction of Pb^{2+} is $Pb^{2+}(aq) + 2e- \rightarrow Pb(s)$. Lead ion in the solution takes two electron and becomes Pb after that the oxidation reaction $Pb(s) \rightarrow Pb^{2+}(aq) + 2e-$ occurs. Lead atom loses electron to become $Pb^{2+}(aq)$ back to the solution.

3.1.3 Cyclic voltammetry of Cd(II) solution at glassy carbon electrode

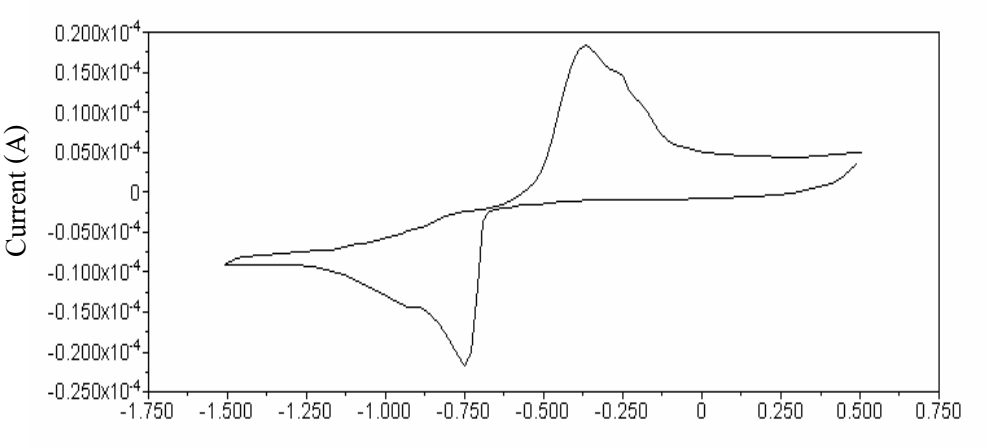

Figure 3-3 Cyclic voltammogram of 112.40 mg L^{-1} Cd(II) at glassy carbon electrode in 50 mL CH_3CN containing 0.1 M TBAP with scan rate of 100 mV s^{-1}

Cyclic voltammogram of Cd(II) is shown in Figure 3-3. These voltammogram was obtained with glassy carbon electrode immersed in 112.40 mg L^{-1} Cd(II) containing CH_3CN and 0.1 M TBAP as electrolyte. The resting potential is -0.353 V. The reduction peak (Epc) appears at -0.750 V vs Ag/AgCl and Ipc = 1.855×10^{-5} A. When the scan is reversed, the oxidation peak (Epa) occurs at -0.370 V vs Ag/AgCl and Ipa = 1.847×10^{-5} A. The reduction reaction of Cd^{2+} is $Cd^{2+}(aq) + 2e^- \rightarrow Cd(s)$. Cadmium ion in the solution takes two electron and becomes Cd after that the oxidation reaction $Cd(s) \rightarrow Cd^{2+}(aq) + 2e^-$ occurs. Cadmium atom loses electron to become $Cd^{2+}(aq)$ back to the solution.

3.1.4 Cyclic voltammetry of Hg(II) solution at glassy carbon electrode

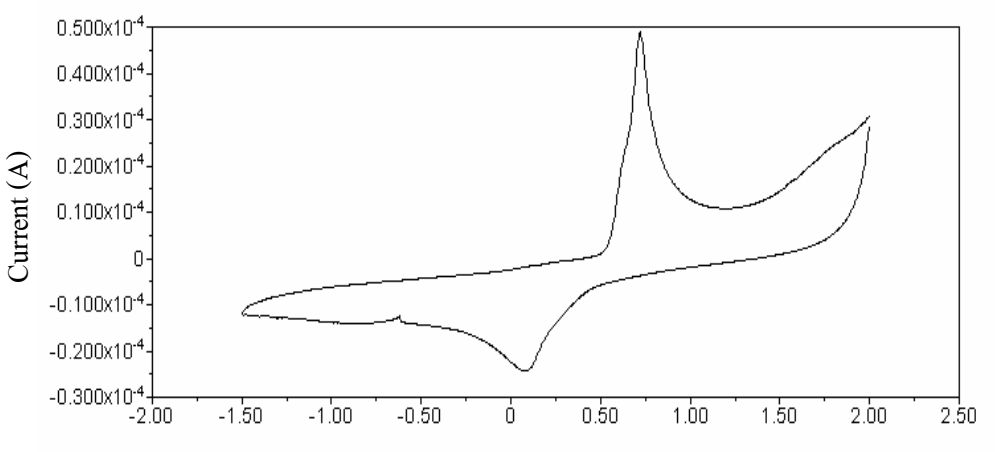

Figure 3-4 Cyclic voltammogram of 200.59 mg L^{-1} Hg(II) at glassy carbon electrode in 50 mL CH_3CN containing 0.1 M TBAP with scan rate of 100 mV s^{-1}

Cyclic voltammogram of 200.59 mg L^{-1} Hg(II) in CH_3CN containing 0.1 M TBAP as electrolyte is shown in Figure 3-4. The resting potential is 0.630 V. The reduction peak (Epc) appears at 0.088 V vs Ag/AgCl and Ipc = 1.614×10^{-5} A. When the scan is reversed, the oxidation peak (Epa) occurs at 0.721 V vs Ag/AgCl and Ipa = 4.494×10^{-5} A. The reduction reaction of Hg^{2+} is $Hg^{2+}(aq) + 2e^- \rightarrow Hg(s)$. Mercury ion in the solution takes two electron and becomes Hg after that the oxidation reaction $Hg(s) \rightarrow Hg^{2+}(aq) + 2e^-$ occurs. Mercury atom loses electron to become $Hg^{2+}(aq)$ back to the solution.

3.1.4 Cyclic voltammetry of Cu(II) solution at glassy carbon electrode

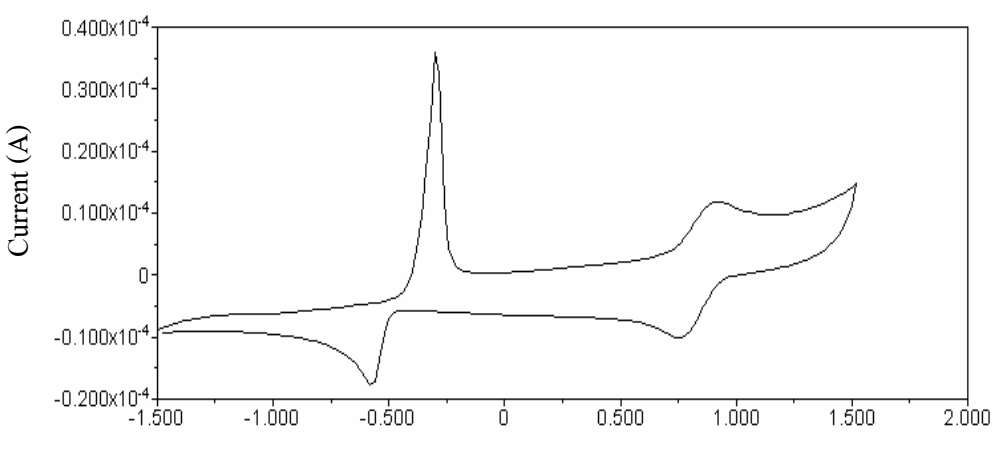

Figure 3-5 Cyclic voltammogram of 63.55 mg L^{-1} Cu(II) at glassy carbon electrode in 50 mL CH_3CN containing 0.1 M TBAP with scan rate of 100 mV s^{-1}

The cyclic voltammogram of 63.55 mg L^{-1} Cu(II) shows two redox couples in CH_3CN and 0.1 M TBAP as in Figure 3-5. The resting potential is 0.976 V. The first redox couple at Epc_1 = 0.759 V vs Ag/AgCl ($Ipc_1 = 9.294 \times 10^{-6}$ A), and Epa_1 = 0.899 V vs Ag/AgCl ($Ipa_1 = 5.632 \times 10^{-6}$ A). This behavior shows the second reduction at Epc_2 = -0.580 V vs Ag/AgCl ($Ipc_2 = 1.130 \times 10^{-5}$ A), and Epa_2 = -0.301 V vs Ag/AgCl ($Ipa_2 = 3.793 \times 10^{-5}$ A). The first reduction reaction is $Cu^{2+}(aq) + e^- \longrightarrow Cu^{+}(aq)$. This is followed by the second reduction of copper(I) to cupper(0), $Cu^{+}(aq) + e^- \longrightarrow Cu^{0}(s)$. When the scan is reversed, the first oxidation reaction is copper(0) to copper(I), $Cu^{0}(s) \longrightarrow Cu^{+}(aq) + e^-$ following the second oxidation of copper(I) to cupper(II), $Cu^{+}(aq) \longrightarrow Cu^{2+}(aq) + e^-$ back to the solution.

3.2 Electrochemical behavior of group of xanthone

3.2.1 Cyclic voltammetry of xanthone at glassy carbon electrode

Cyclic voltammogram of 1 mM xanthone in CH_3CN containing 0.1 M TBAP as electrolyte is shown in Figure 3-6. Xanthone exhibits two steps of reduction. The first reduction peak occurs at -1.720 V vs Ag/AgCl ($Ipc_1 = 8.369 \times 10^{-6}$ A) and oxidation peak is -1.640 V vs Ag/AgCl ($Ipa_1 = 5.1034 \times 10^{-6}$ A). The redox couple exhibits not completely chemically reversible ($Ipa_1 / Ipc_1 \neq 1$). There is one independence reduction peak which occurs at -2.260 V vs Ag/AgCl ($Ipc_2 = 4.968 \times 10^{-6}$ A). This peak is electrochemical irreversible and no oxidation couple.

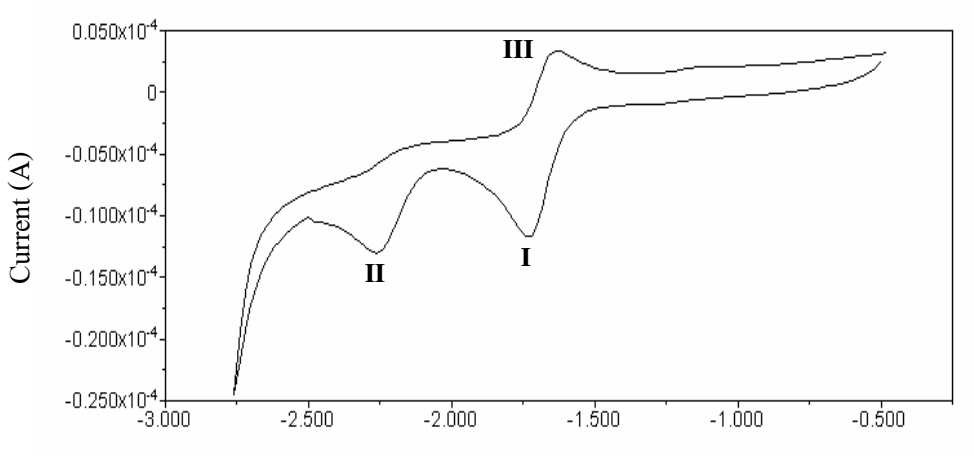

Figure 3-6 Cyclic voltammogram of 1 mM xanthone at glassy carbon electrode in 50 mL CH_3CN containing 0.1 M TBAP with scan rate of 100 mV s^{-1} and resting potential is -0.021 V

The first electrochemically quasi-reversible couple (I, III) is due to the reduction of carbonyl group.

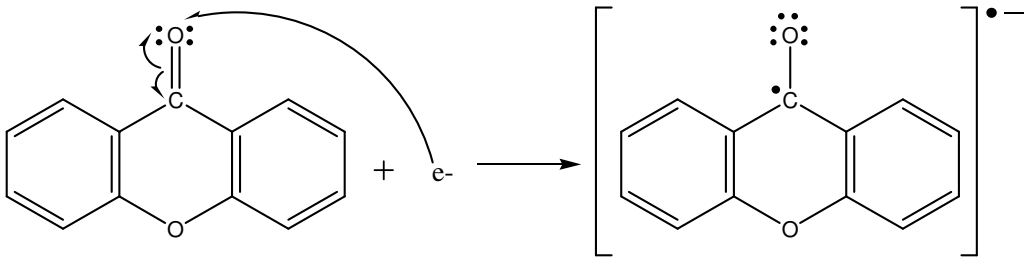

xanthone Ketyl radical anion

The ketyl radical anion can be reduced to from dianion in the second reduction step.

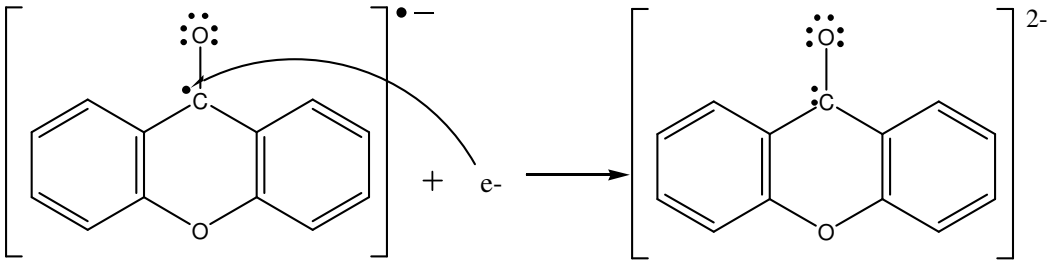

Ketyl radical anion Dianion

3.2.2 Cyclic voltammetry of thioxanthone at glassy carbon electrode

Cyclic voltammogram of 1 mM thioxanthone in CH_3CN containing 0.1 M TBAP as electrolyte is shown in Figure 3-7. The electrochemical behavior of thioxanthone is so much similar to that xanthone which exhibits two steps of reduction. The first redox couple at Ecp_1 = -1.660 V vs Ag/AgCl ($Ipc_1 = 6.595 \times 10^{-6}$ A) and Epa_1 = -1.581 V vs Ag/AgCl ($Ipa_1 = 4.114 \times 10^{-6}$ A). The redox couple exhibits not completely chemically reversible (Ipa1/Ipc1 ≠ 1). There is one independence reduction peak which occurs at Epc_2 = -2.100 V vs Ag/AgCl ($Ipc_2 = 3.919 \times 10^{-6}$ A). This peak is electrochemically irreversible and is no oxidation couple.

The first electrochemically quasi-reversible couple (I, III) is due to the reduction of carbonyl group. The ketyl radical anion can be reduced to from dianion in the second reduction step.

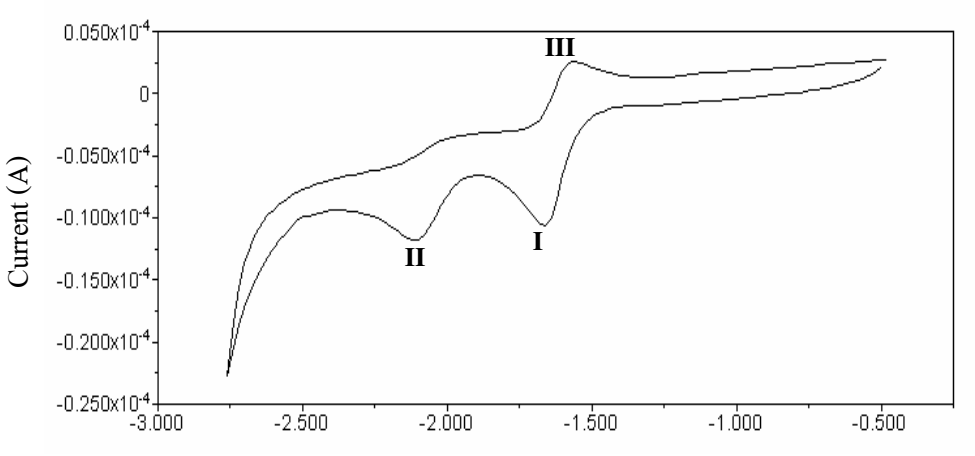

Figure 3-7 Cyclic voltammogram of 1 mM thioxanthone at glassy carbon electrode in 50 mL CH_3CN containing 0.1 M TBAP with scan rate of 100 mV s^{-1} and resting potential is -0.357 V

3.2.3 Cyclic voltammetry of xanthene at glassy carbon electrode

Cyclic voltammogram of 1 mM xanthene was performed in the potential window of -3.000 V to 1.000 V vs Ag/AgCl which there is no peak, indicating that there is no redox reaction at glassy carbon electrode as shown in Figure 3-8.

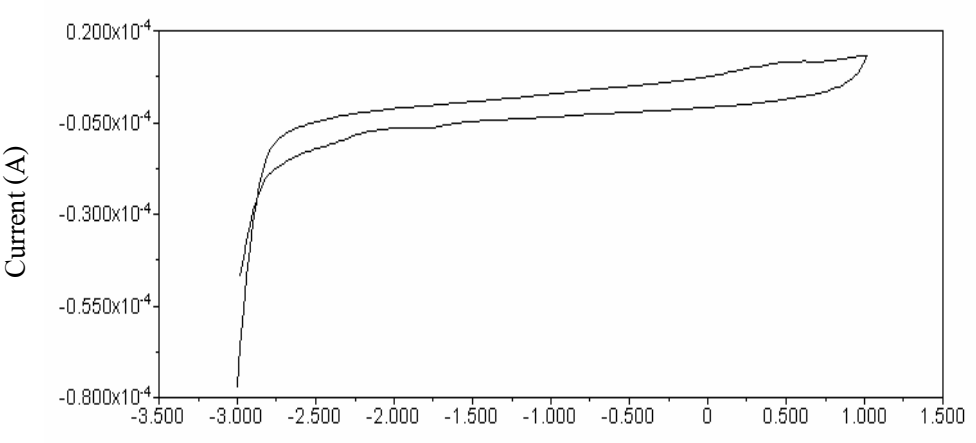

Figure 3-8 Cyclic voltammogram of 1 mM xanthene at glassy carbon electrode in 50 mL CH_3CN containing 0.1 M TBAP with scan rate of 100 mV s^{-1} and resting potential is -0.374 V

3.2.4 Cyclic voltammetry of acridone at glassy carbon electrode

Cyclic voltammogram of 1 mM acridone was performed in the potential window of -2.500 V to 2.000 V vs Ag/AgCl which there is no peak, indicating that there is no redox reaction at glassy carbon electrode as shown in Figure 3-9.

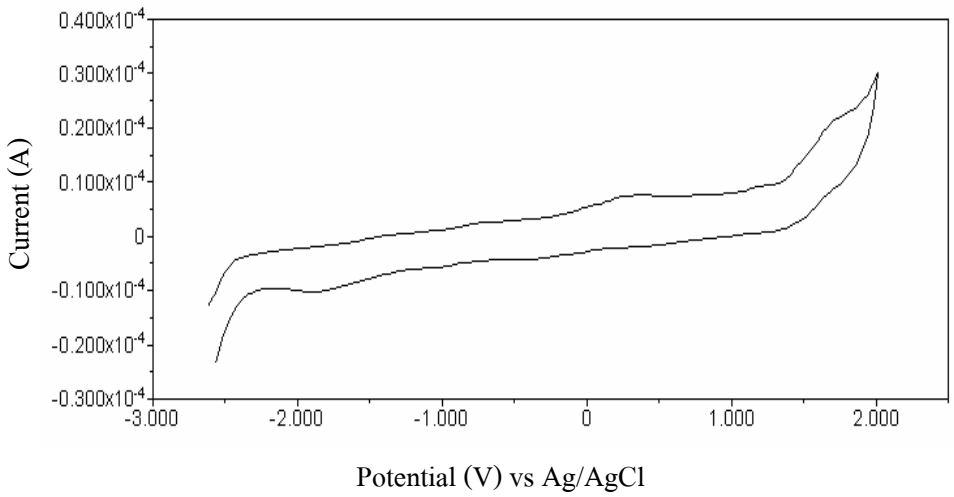

Figure 3-9 Cyclic voltammogram of 1 mM acridone at glassy carbon electrode in 50 mL CH_3CN containing 0.1 M TBAP with scan rate of 100 mVs^{-1} and resting potential is -0.350 V

From the results of cyclic voltammetry could be summarized the peak potentials and the peak currents of metal and group of xanthone compounds as shown in Table 3-1 – 3-2.

Table 3-1 The peak potentials and the peak currents of metal in CH_3CN

Metal	Epc (V)	Epa (V)	Ipc (A)	Ipa (A)
207.20 mg L^{-1} Pb(II)	-0.548	-0.460	1.985×10^{-6}	1.740×10^{-6}
112.40 mg L^{-1} Cd(II)	-0.750	-0.370	1.855×10^{-5}	1.847×10^{-5}
200.59 mg L^{-1} Hg(II)	0.088	0.721	1.614×10^{-5}	4.494×10^{-5}
63.55 mg L^{-1} Cu(II)	0.759 -0.580	0.899 -0.301	9.294×10^{-6} 1.130×10^{-5}	5.632×10^{-6} 3.793×10^{-5}

Table 3-2 The peak potentials and the peak currents of group of xanthone compounds in CH_3CN

Group of xanthone compounds	Epc (V)	Epa (V)	Ipc (A)	Ipa (A)
1 mM xanthone	-1.720 -2.260	-1.640 -	8.369×10^{-6} 4.968×10^{-6}	5.1034×10^{-6}
1 mM thioxanthone	-1.660 -2.100	-1.581	6.595×10^{-6} 3.919×10^{-6}	4.114×10^{-6}
1 mM xanthene	No peak	No peak	-	-
1 mM acridone	No peak	No peak	-	-

3.3 Stripping voltammetry of Cd(II), Cu(II), Hg(II) and Pb(II) by carbon paste electrode

3.3.1 Effect of electrolyte for determination of Cd(II), Cu(II), Hg(II) and Pb(II) by unmodified electrode

The effect of electrolyte for determination of Cd(II), Cu(II), Hg(II) and Pb(II) at unmodified electrode are shown in Table 3-3 – 3-6 and Figure 3-10 – 3-13.

Table 3-3 Effects of electrolyte on the peak current of 10 mg L^{-1} Cd(II) at unmodified electrode

Electrolyte	Current $\times 10^{-5}$(A)
0.2 HNO_3	0.000
0.2 M acetate buffer (pH5)	2.275
0.3 M CH_3COONH_4	7.466
0.2 M CH_3COONa	5.985

* 3 replications, RSD $\leq$ 6%

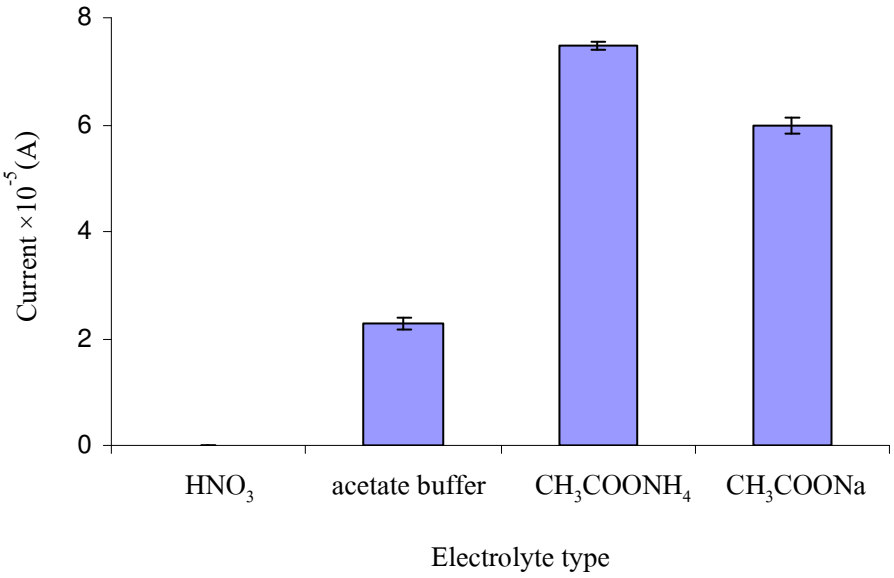

Figure 3-10 Effects of electrolyte on the peak current of 10 mg L^{-1} Cd(II) at unmodified electrode

Table 3-4 Effects of electrolyte on the peak current of 10 mg L^{-1} Cu(II) at unmodified electrode

Electrolyte	Current $\times 10^{-5}$(A)
0.2 HNO_3	0.000
0.2 M acetate buffer (pH5)	24.409
0.3 M CH_3COONH_4	0.000
0.2 M CH_3COONa	16.172

* 3 replications, RSD ≤ 6%

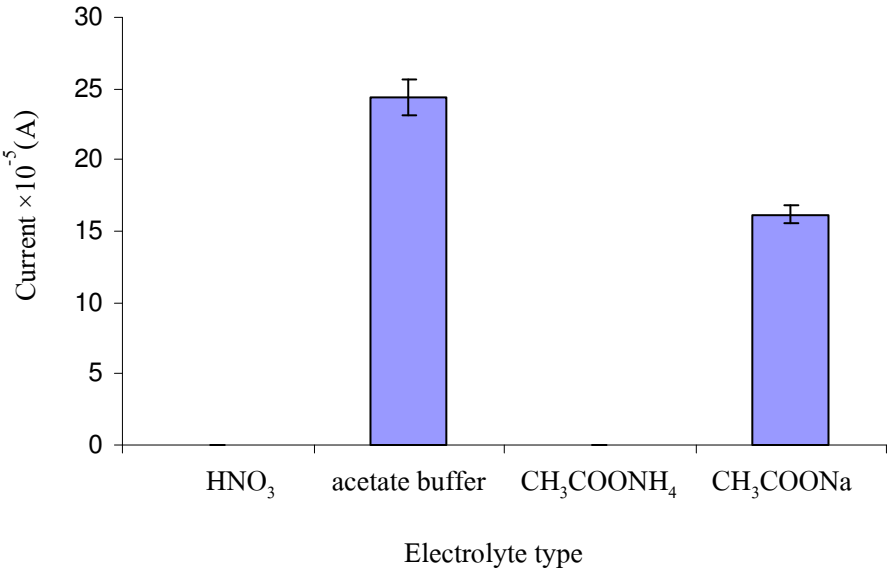

Figure 3-11 Effects of electrolyte on the peak current of 10 mg L^{-1} Cu(II) at unmodified electrode

Table 3-5 Effects of electrolyte on the peak current of 10 mg L^{-1} Hg(II) at unmodified electrode

Electrolyte	Current $\times 10^{-5}$(A)
0.2 HNO_3	0.000
0.2 M acetate buffer (pH5)	7.405
0.3 M CH_3COONH_4	0.000
0.2 M CH_3COONa	2.977

* 3 replications, RSD ≤ 5%

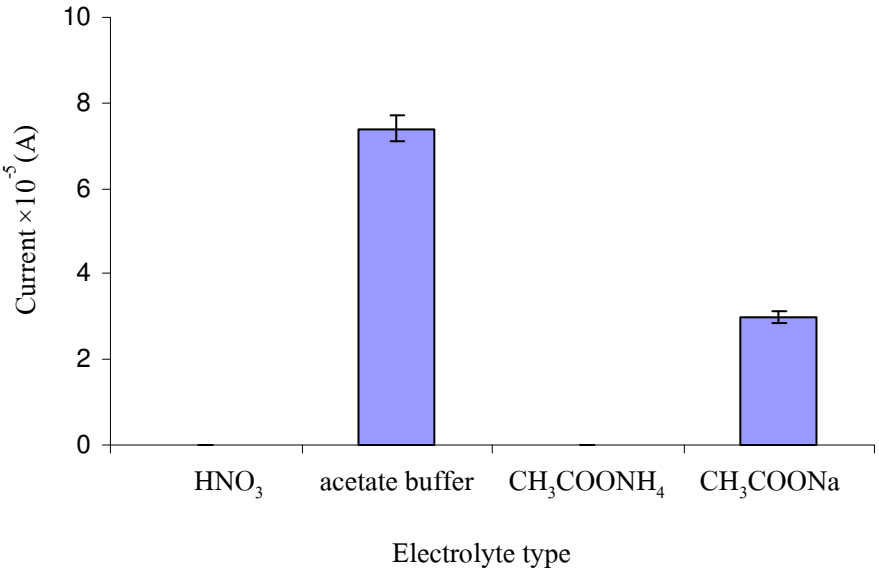

Figure 3-12 Effects of electrolyte on the peak current of 10 mg L^{-1} Hg(II) at unmodified electrode

Table 3-6 Effects of electrolyte on the peak current of 10 mg L^{-1} Pb(II) at unmodified electrode

Electrolyte	Current $\times 10^{-5}$(A)
0.2 HNO_3	84.816
0.2 M acetate buffer (pH5)	11.546
0.3 M CH_3COONH_4	4.567
0.2 M CH_3COONa	12.963

* 3 replications, RSD $\leq$ 6%

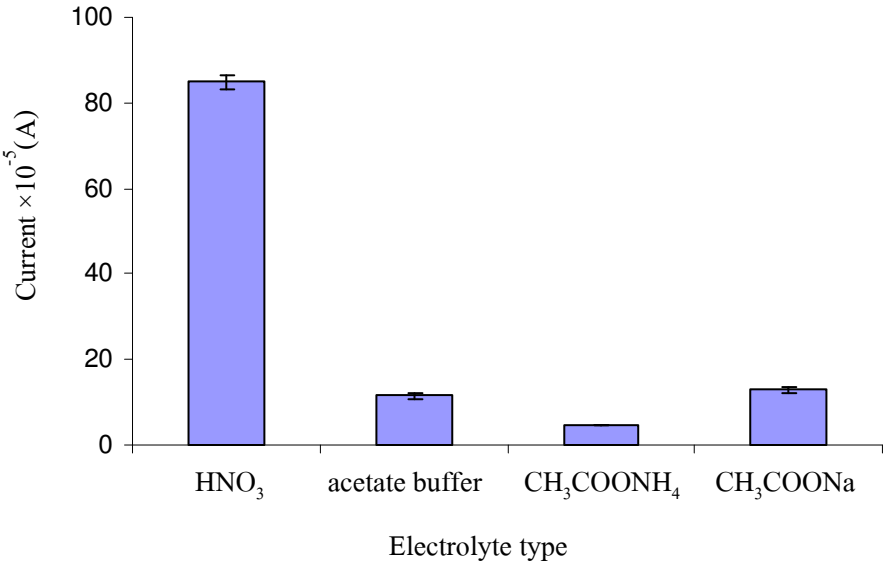

Figure 3-13 Effects of electrolyte on the peak current of 10 mg L^{-1} Pb(II) at unmodified electrode

From the results obtained in Table 3-3 – 3-6 and Figure 3-10 – 3-13, it can be concluded that the highest peak heights of Cd(II), Cu(II), Hg(II) and Pb(II) were achieved in 0.3 M CH_3COONH_4, 0.2 M acetate buffer, 0.2 M acetate buffer and 0.2 HNO_3 solution, respectively. Thus, those electrolytes mentioned above were used as electrolyte further experiment.

3.3.2 Stripping voltammetry of Cd(II), Cu(II), Hg(II) and Pb(II) by carbon paste electrode modified with group of xanthone compounds

Stripping voltammograms of metal were obtained at unmodified and group of xanthone compounds modified carbon paste electrode (modifier/ graphite power 7.5% and 15% (w/w)). The concentration of 5 mg L^{-1} Cd(II) in 0.3 M CH_3COONH_4 was measured after preconcentration for 2 min at the potential of -1.10 V. The stripping voltammogram was recorded form -1.10 to -0.70 V. The peak was observed at -0.85 V. The responses of current from voltammograms on unmodified CPE compared with the modified CPE are shown in Table 3-7 and Figure 3-14. The stripping voltammogram of Cd(II) was the example of the signals obtained at unmodified and modified electrode with xanthone, as shown in Figure 3-15.

Stripping voltammograms of 5 mg L^{-1} Cu(II) in 0.2 M acetate buffer was measured after preconcentration for 2 min at the potential of -0.30 V. The stripping voltammogram was recorded form -0.30 to 0.10 V. The peak was observed at 0.01 V. The responses of current from voltammograms on unmodified CPE compared with the modified CPE are shown in Table 3-8 and Figure 3-16. The stripping voltammogram of Cu(II) was the example of the signals obtained at unmodified and modified electrode with xanthone, as shown in Figure 3-17.

Stripping voltammograms of 10 mg L^{-1} Hg(II) in 0.2 M acetate buffer was measured after preconcentration for 1 min at the potential of -0.30 V. The stripping voltammogram was recorded from -0.30 to 0.50 V. The peak was observed at 0.28 V. The responses of current from voltammograms on unmodified CPE compared with the modified CPE are shown in Table 3-9 and Figure 3-18. The stripping voltammogram of Hg(II) was the example of the signals obtained at unmodified and modified electrode with xanthone, as shown in Figure 3-19.

Stripping voltammograms of 5 mg L^{-1} Pb(II) in 0.2 M $HNO_3$was measured after preconcentration for 1 min at the potential of -0.70 V. The stripping voltammogram was recorded form -0.70 to -0.30 V. The peak was observed at -0.55 V. The responses of current from voltammograms on unmodified CPE compared with the modified CPE are shown in Table 3-10 and Figure 3-20. The stripping voltammogram of Pb(II) was the example of the signals obtained at unmodified and modified electrode with xanthone, as shown in Figure 3-21.

From this experiment the results were shown that the peak current of group of xanthone compounds modified CPE are lower than unmodified CPE. It can be concluded that group of xanthone compounds is not suitable for quantitative analysis of these metals at studied condition.

In 2005, Photicunapat modified CPE electrode with xanthone for determination of silver. It was found that xanthone can be used to increase the sensitivity of the determination of silver because xanthone has more positive first reduction potential shows better affinity to silver (Photicunapat, 2005). Therefore, modifier should be used as additional function group such as –OH for binding metal in further project.

Table 3-7 The current from stripping voltammogram of 5 mg L^{-1} Cd(II) in 0.3 M CH_3COONH_4 at various group of xanthone compounds

Compounds	Current $\times 10^{-5}$(A)	
	7.5% (w/w)	15%(w/w)
unmodified	12.153	
xanthone	6.550	2.791
xanthene	3.351	7.298
Thioxanthone	7.313	5.162
acridone	7.536	6.451

* 3 replications, RSD ≤ 8.2%

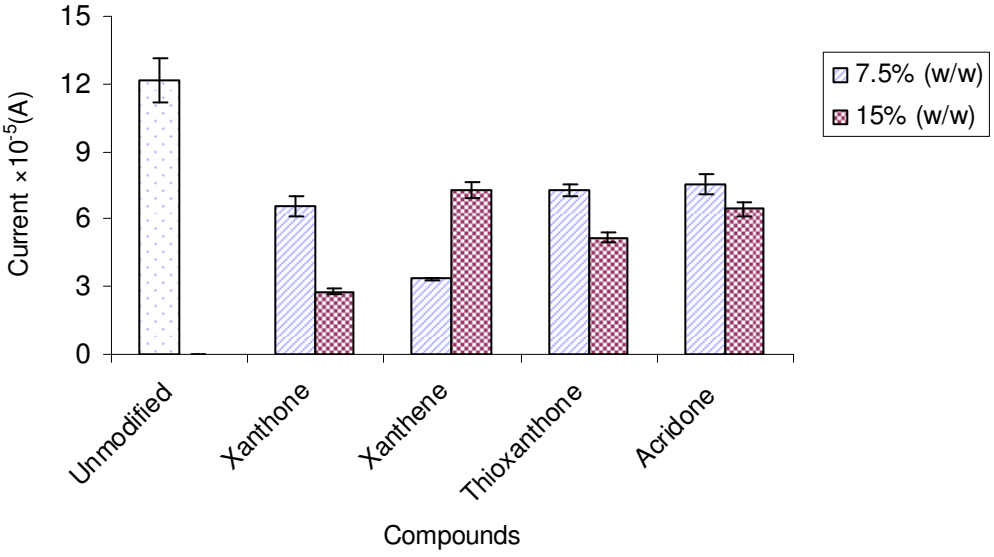

Figure 3-14 The current from stripping voltammogram of 5 mg L^{-1} Cd(II) in 0.3 M CH_3COONH_4 at various group of xanthone compounds

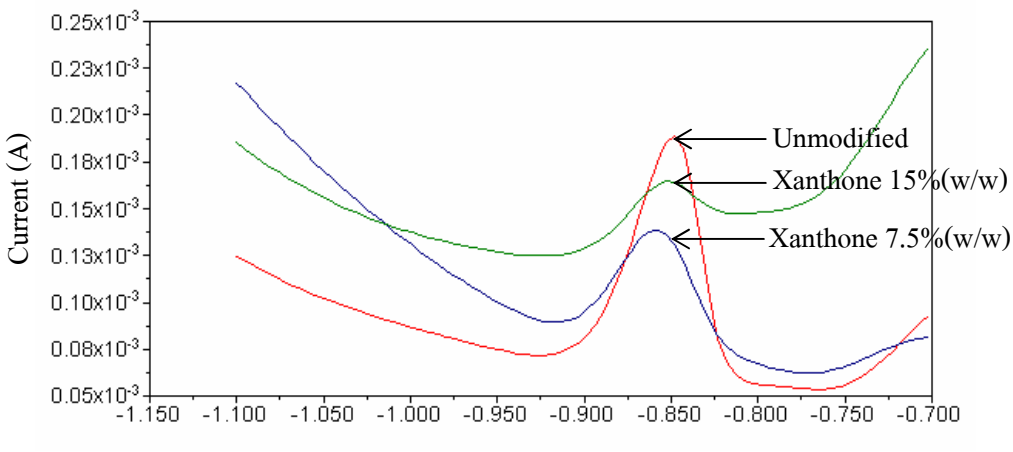

Figure 3-15 Stripping voltammogram of 5 mg L^{-1} Cd(II) in 0.3 M CH_3COONH_4 at unmodified and modified electrode with xanthone compound

Table 3-8 The current from stripping voltammogram of 5 mg L^{-1} Cu(II) in 0.2 M acetate buffer at various group of xanthone compounds

Compounds	Current $\times 10^{-5}$(A)	
	7.5% w/w	15% w/w
unmodified	9.427	
xanthone	2.823	2.253
xanthene	4.298	1.614
Thioxanthone	5.018	2.719
acridone	2.644	2.233

* 3 replications, RSD $\leq$ 8%

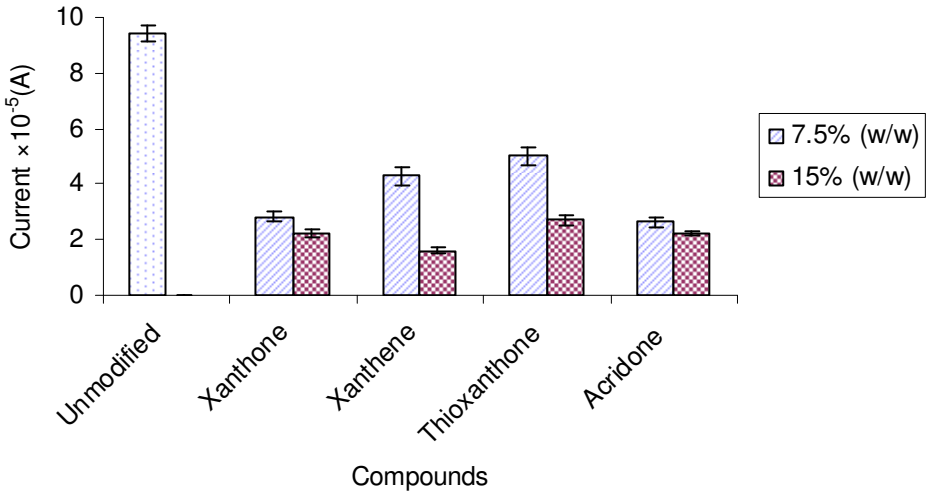

Figure 3-16 The current from stripping voltammogram of 5 mg L^{-1} Cu(II) in 0.2 M acetate buffer at various group of xanthone compounds

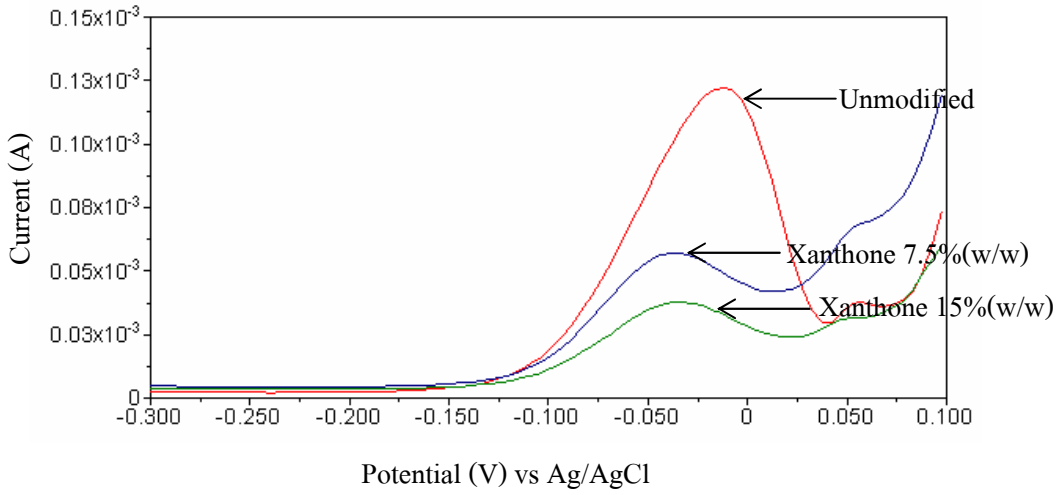

Figure 3-17 Stripping voltammogram of 5 mg L^{-1} Cu(II) in 0.2 M acetate buffer at unmodified and modified electrode with xanthone compound

Table 3-9 The current from stripping voltammogram of 10 mg L^{-1} Hg(II) in 0.2 M acetate buffer at various group of xanthone compounds

Compounds	Current $\times 10^{-5}$(A)	
	7.5% w/w	15% w/w
unmodified	4.343	
xanthone	4.065	3.498
xanthene	1.854	1.613
Thioxanthone	2.479	1.669
acridone	2.533	2.352

* 3 replications, RSD $\leq$ 8%

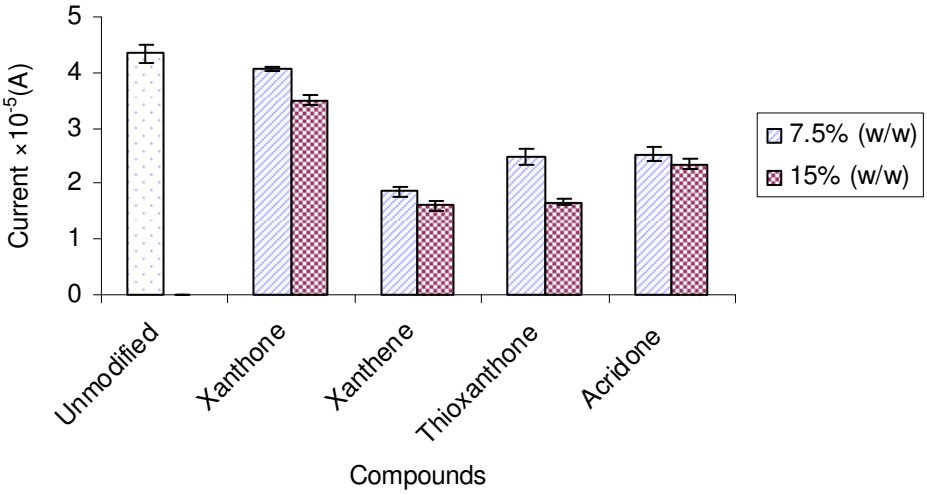

Figure 3-18 The current from stripping voltammogram of 10 mg L^{-1} Hg(II) in 0.2 M acetate buffer at various group of xanthone compounds

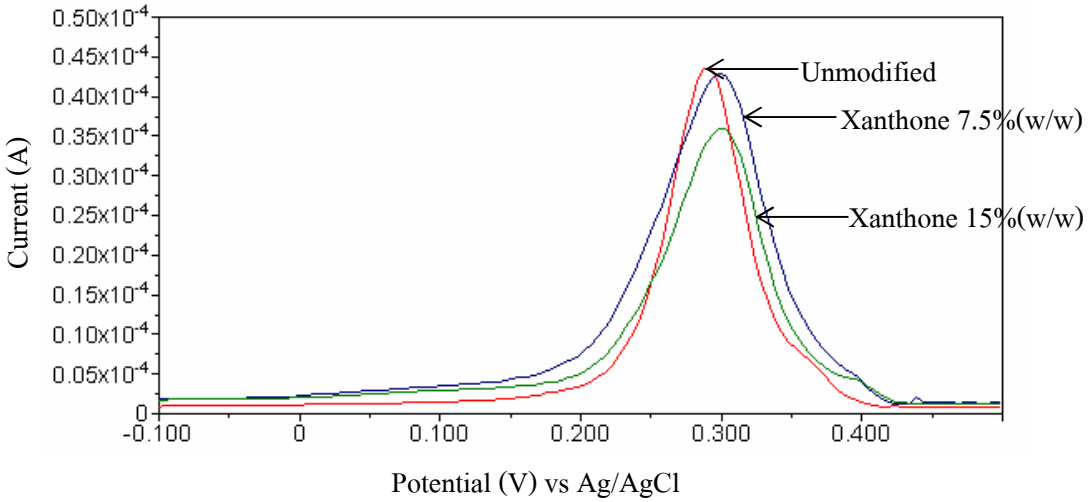

Figure 3-19 Stripping voltammogram of 10 mg L^{-1} Hg(II) in 0.2 M acetate buffer at unmodified and modified electrode with xanthone compound

Table 3-10 The current from stripping voltammogram of 5 mg L^{-1} Pb(II) in 0.2 M HNO_3 at various group of xanthone compounds

compounds	Current $\times 10^{-5}$(A)	
	7.5% w/w	15% w/w
unmodified	31.382	
xanthone	18.756	20.445
xanthene	22.706	17.766
Thioxanthone	13.474	5.475
acridone	19.514	16.182

* 3 replications, RSD $\leq$ 5%

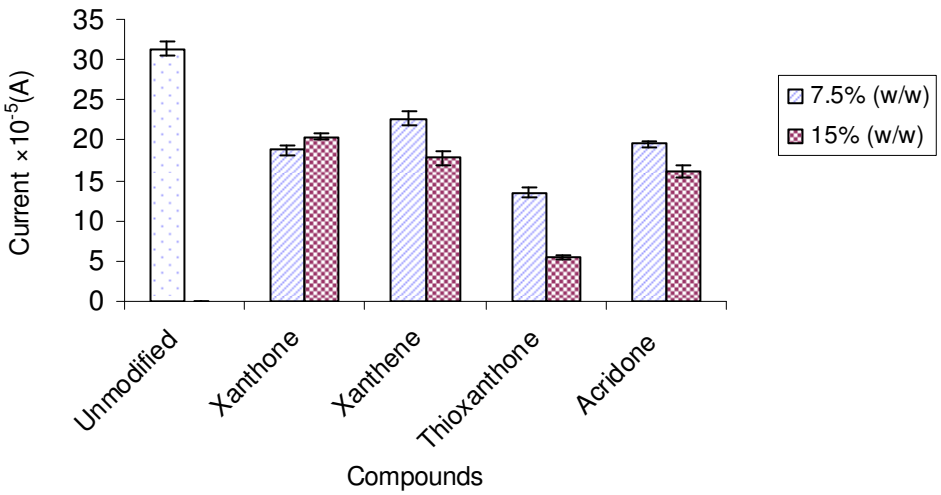

Figure 3-20 The current from stripping voltammogram of 5 mg L^{-1} Pb(II) in 0.2 M HNO_3 at various group of xanthone compounds

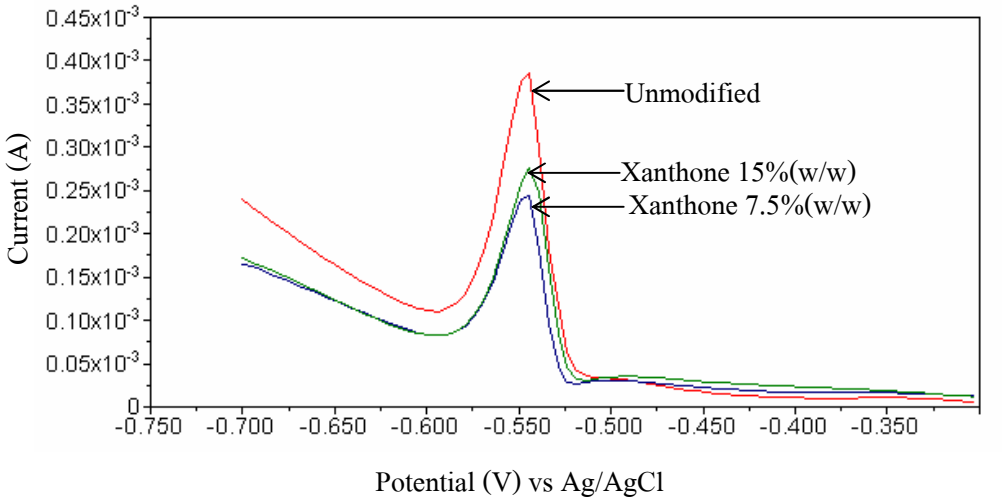

Figure 3-21 Stripping voltammogram of 5 mg L^{-1} Pb(II) in 0.2 M HNO_3 at unmodified and modified electrode with xanthone compound

3.4 Optimization condition for determination Pb(II) by adsorptive stripping voltammetry

3.4.1 Adsorptive characteristics of the Pb-8-hydroxyquinoline complex

Preliminary experiments were performed to characterize the suitability of 8-hydroxyquinoline for the determination of lead ion using HMDE. Figure 3-22 displays stripping voltammogram of 0.1 mM 8-hydroxyquinoline solution in 0.01 M ammonium acetate at pH = 8.0 after 1 min accumulation at -0.4 V. Figure 3-23 shows the stripping voltammogram of solution containing 1 mg L^{-1} Pb(II) in the absence of 8-hydroxyquinoline ligand under condition similar to those in Figure 3-22. Figure 3-24 shows the stripping voltammogram of mixture of 0.1 mM 8-hydroxyquinoline and 1 mg L^{-1} Pb(II) in 0.01 M ammonium acetate at pH = 8.0 after 1 min accumulation at -0.4 V. It had found reduction peak at -0.578 V (Figure 3-24). It can be concluded that the sensitivity of lead reduction currents enhanced due to the addition of 8-hydroxyquinoline to the solution. Indicate that the Pb-8-hydroxyquinoline complex was adsorbed on the surface of electrode.

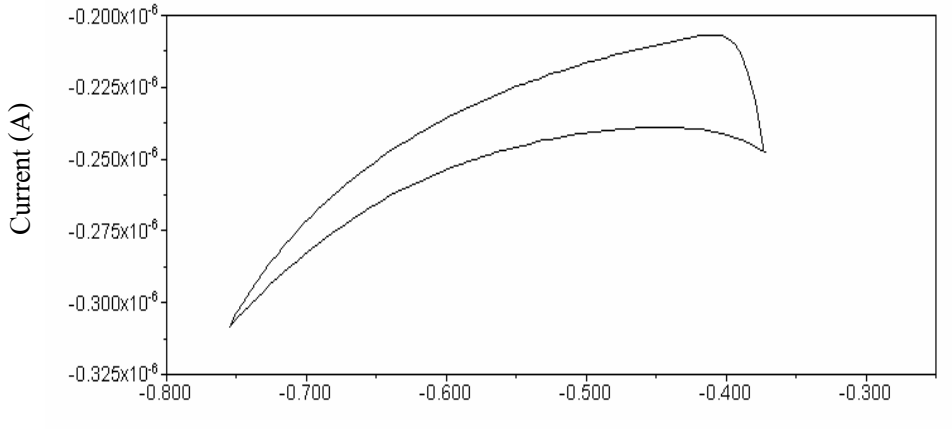

Figure 3-22 Stripping voltammogram of the 0.1 mM 8-hydroxyquinoline in 0.01 M ammonium acetate at pH = 8.0 after 1 min accumulation at -0.4 V and scan rate of 50 mV s^{-1}

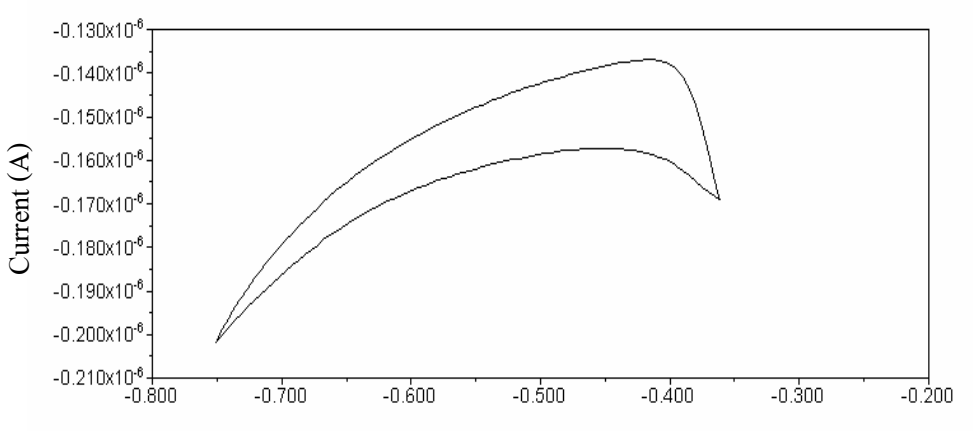

Figure 3-23 Stripping voltammogram of the 1 mg L^{-1} Pb(II) in 0.01 M ammonium acetate at pH = 8.0 after 1 min accumulation at -0.4 V and scan rate of 50 mV s^{-1}

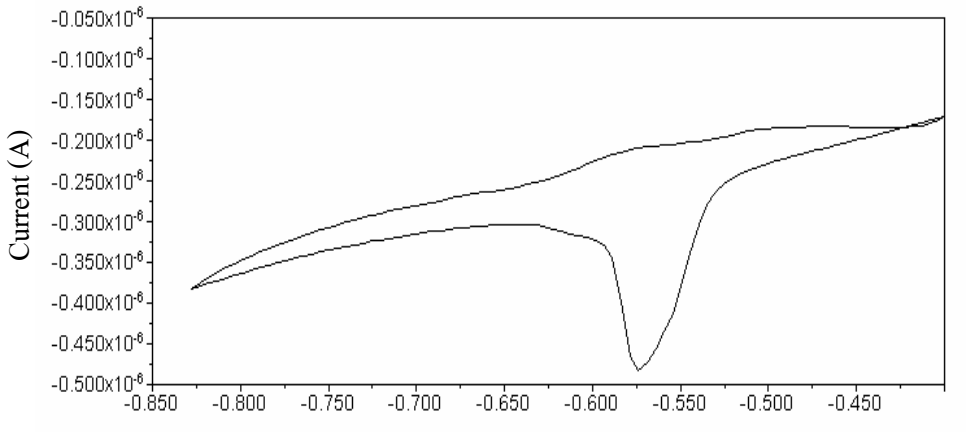

Figure 3-24 Stripping voltammogram of mixture of 0.1 mM 8-hydroxyquinoline and 1 mg L^{-1} Pb(II) in 0.01 M ammonium acetate at pH = 8.0 after 1 min accumulation at -0.4 V and scan rate of 50 mV s^{-1}

3.4.2 Comparison of square wave versus differential pulse

A number of different wave forms have been used for the stripping step, including linear sweep voltammetry (LSV), differential pulse voltammetry (DPV), and square wave voltammetry (SWV). SWV and DPV are more commonly used, due to their lower detection limits (Buffle and Tercier-Waeber, 2005).

A comparison of the sensitivities for lead analysis between square wave and differential pulse is shown in Table 3-11 and Figure 3-25. It was found that the sensitivity of square wave was higher than differential pulse. Thus, square wave was selected for all experiments.

Table 3-11 The comparison of peak current between square wave and differential pulse of Pb(II) in 0.01 M ammonium acetate containing 10 μM 8-hydroxyquinoline at pH = 8.0

Pb(II) Concentration ($\mu g\ L^{-1}$)	Current $\times 10^{-8}$(A)	
	SW	DP
0	0	0
5	2.189	0.249
10	4.614	0.557
15	6.991	0.784
20	9.442	1.092

* 3 replications, RSD $\leq$ 4%

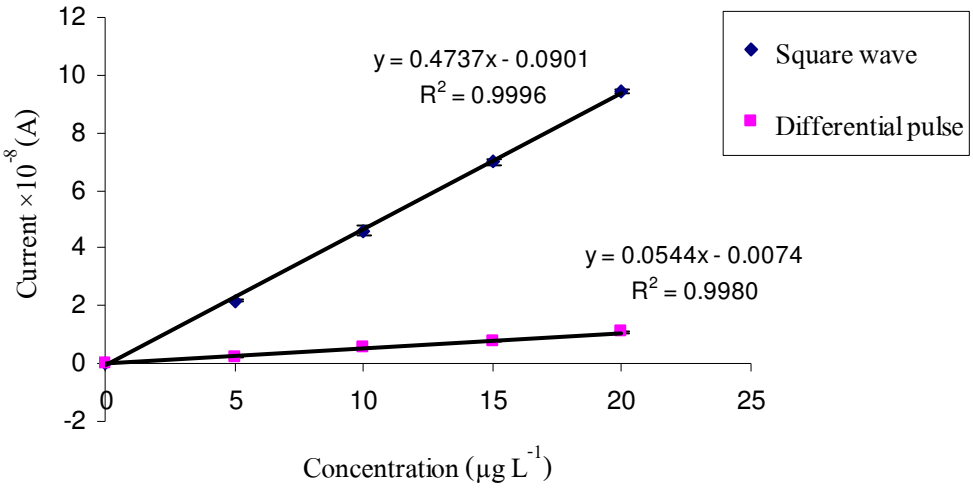

Figure 3-25 The comparison of peak current between square wave and differential pulse of Pb(II) in 0.01 M ammonium acetate containing 10 µM 8-hydroxyquinoline at pH = 8.0

3.4.3 Comparison of peak height versus peak area

A comparison of sensitivities for signal measurements between peak height and peak area was shown in Table 3-12 and Figure 3-26.

Table 3-12 The comparison of peak height and peak area of Pb(II) in 0.01 M ammonium acetate containing 10 µM 8-hydroxyquinoline at pH = 8.0

Pb(II) Concentration ($\mu g\ L^{-1}$)	Current × 10^{-8}(A)	
	Peak height	Peak area
0	0	0
5	2.189	0.111
10	4.614	0.256
15	6.991	0.394
20	9.442	0.577

* 3 replications, RSD ≤ 6%

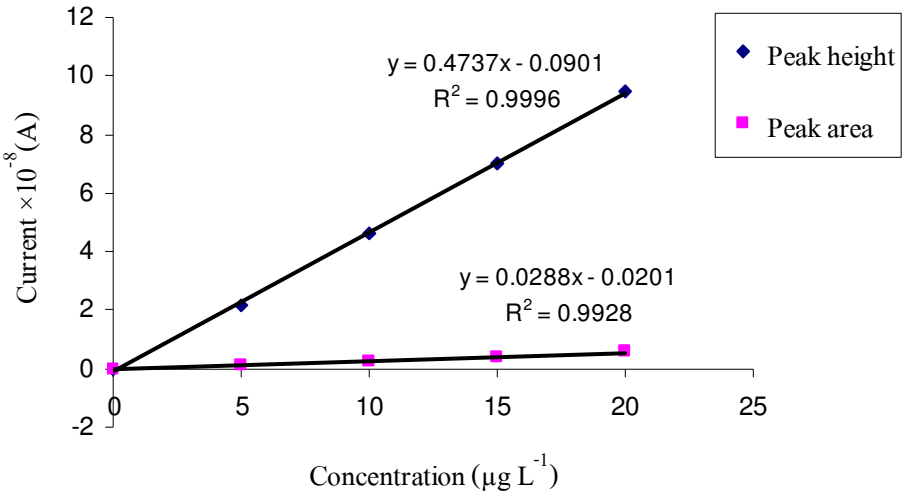

Figure 3-26 The comparison of peak height and peak area of Pb(II) in 0.01 M ammonium acetate containing 10 µM 8-hydroxyquinoline at pH = 8.0

It can be concluded from Table 3-12 and Figure 3-26 that the sensitivity of peak height was higher than peak area. Therefore, peak height was selected for signal measurements.

3.4.4 Effect of supporting electrolyte

Electrochemical measurements are commonly carried out in a medium that consists of a supporting electrolyte. Supporting electrolytes are required in controlled-potential experiments to decrease the resistance of the solution, and to maintain a constant ionic strength (Wang, 2000). The effect of difference supporting electrolyte in 0.01 M of CH_3COONH_4, CH_3COONa, Tris, KNO_3 and $NaNO_3$ is shown in Table 3-13 and Figure 3-27.

Table 3-13 Effects of supporting electrolyte on the peak current of 20 µg L^{-1} Pb(II) in the presence of 10 µM 8-hydroxyquinoline at pH = 8.0

Electrolyte	Current $\times 10^{-8}$(A)
0.01 M CH_3COONH_4	9.285
0.01 M CH_3COONa	6.433
0.01 M Tris	7.076
0.01 M KNO_3	7.155
0.01 M $NaNO_3$	6.679

* 3 replications, RSD $\leq$ 4%

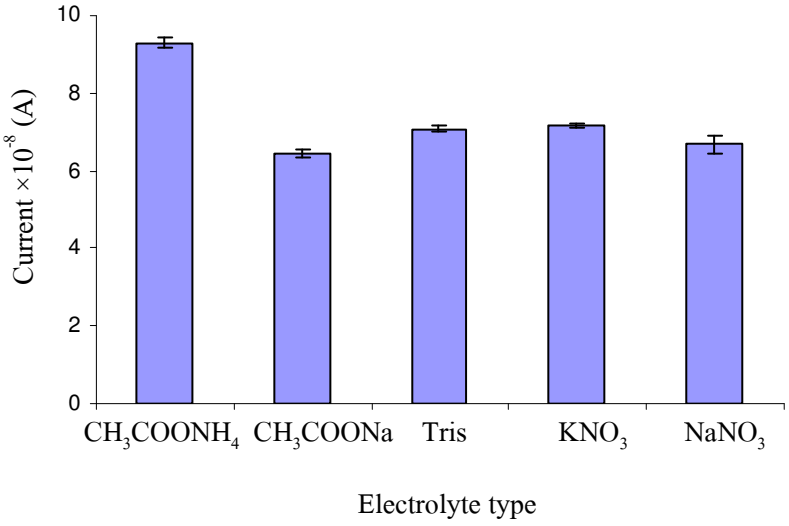

Figure 3-27 Effects of supporting electrolyte on the peak current of 20 µg L^{-1} Pb(II) in the presence of 10 µM 8-hydroxyquinoline at pH = 8.0

The effects of supporting electrolytes were carried out with different types such as CH_3COONH_4, CH_3COONa, Tris, KNO_3 and $NaNO_3$. The highest peak height was achieved in CH_3COONH_4 solution. Thus, CH_3COONH_4 was used as supporting electrolyte for further experiments.

3.4.5 Effect of supporting electrolyte concentration

The effect of concentration of the supporting electrolyte on the stripping peak current of lead was studied by varying the concentration of ammonium acetate in the range 0.01-0.5 M at constant pH (Table 3-14 and Figure 3-28).

Table 3-14 Effects of supporting electrolyte concentration on the peak current of 20 μg L^{-1} Pb(II) in the presence of 10 μM 8-hydroxyquinoline at pH = 8.0

CH_3COONH_4 Concentration (M)	Current $\times 10^{-8}$(A)
0.01	8.687
0.05	8.738
0.10	9.875
0.2	8.597
0.3	8.233
0.4	7.515
0.5	7.298

* 3 replications, RSD ≤ 4%

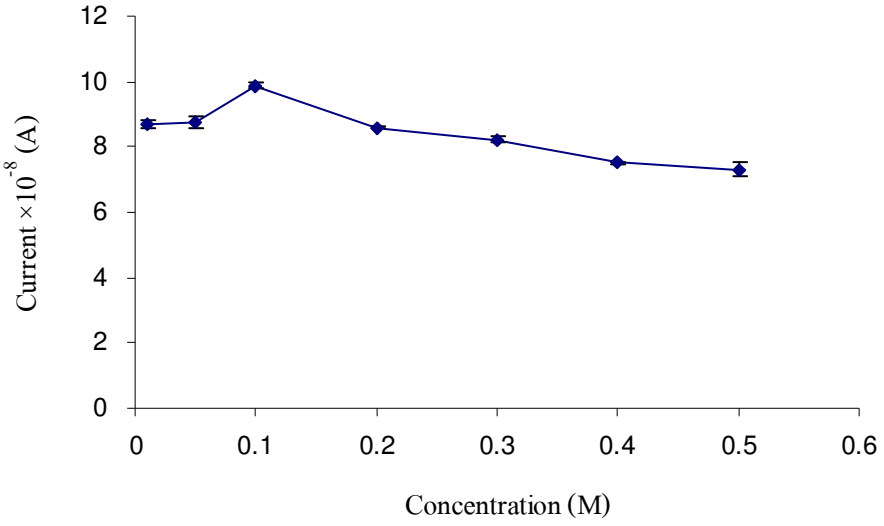

Figure 3-28 Effects of supporting electrolyte concentration on the peak current of 20 μg L^{-1} Pb(II) in the presence of 10 μM 8-hydroxyquinoline at pH = 8.0

The results in Table 3-14 and Figure 3-28 indicated that the maximum peak current was observed for 0.1 M ammonium acetate. It was found that increasing the concentration of ammonium acetate decreased the peak current. This is due the formation of a weak complex between acetate with Pb(II) (Degefa *et al*., 1999)**.** Consequently an optimum ammonium acetate concentration of 0.1M was selected for the next experiments.

3.4.6 Effect of pH

The influence of pH on the stripping peak current of lead was studied in the pH range 6.00 - 7.00. The results are shown in Table 3-15 and Figure 3-29**.**

Table 3-15 Effects pH on the peak current of 20 μg L^{-1} Pb(II) in 0.1 M ammonium acetate containing 10 μM 8-hydroxyquinoline

pH	Current $\times 10^{-8}$ (A)
6.00	0.000
6.50	0.222
7.00	12.549
7.50	12.912
8.00	11.790
8.50	9.634
9.00	9.628
9.50	8.696
10.00	7.890

* 3 replications, RSD $\leq$ 7%

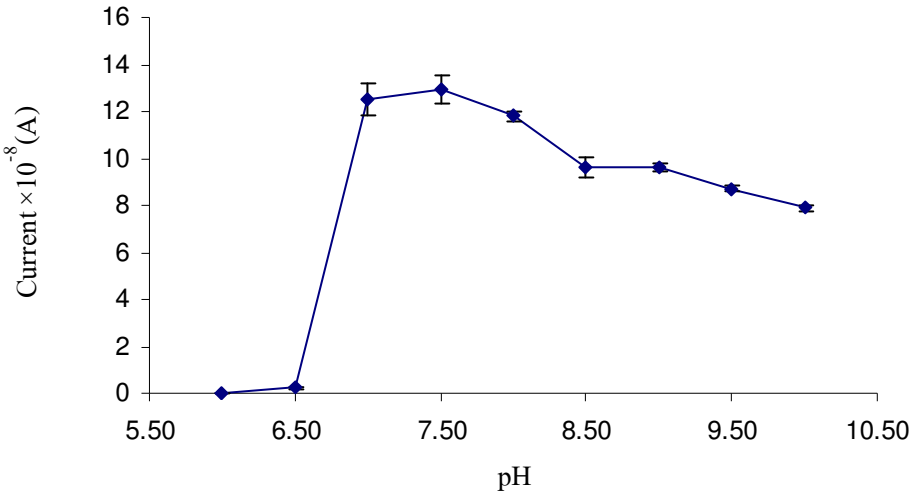

Figure 3-29 Effects pH on the peak current of 20 µg L^{-1} Pb(II) in 0.1 M ammonium acetate containing 10 µM 8-hydroxyquinoline

The results are shown in Table 3-15 and Figure 3-29 which indicate that with a pH range of 6.00 to 7.50 the peak current of the lead complex increased by increasing pH and then decreased by changing pH from 8.00 to 10.00. Thus a pH of 7.50 was chosen for further studies.

At very low pH, the protonation of -NH groups (in 8-hydroxyquinoline) (Lapinee, 2006) and at high pH, hydrolysis of Pb(II) which would increasingly affect the formation of Pb(II)-8-hydroxyquinoline complexes (Jurado-González *et .al.,* 2003). Therefore, at low and high pH the complexation of 8-hydroxyquinoline with Pb(II) ions will decrease.

3.4.7 Effect of 8-hydroxyquinoline concentration

The effect of the 8-hydroxyquinoline concentration on the cathodic stripping peak current of 20 µg L^{-1} Pb(II) in 0.1 M ammonium acetate at pH 7.5 with a accumulation potential of -1.1 V for 60 s is shown in Table 3-16 and Figure 3-30.

Table 3-16 Effects of 8-hydroxyquinoline concentration on the peak current of 20 μg L^{-1} Pb(II) in 0.1 M ammonium acetate at pH = 7.5

8-hydroxyquinoline Concentration (μM)	Current $\times 10^{-8}$(A)
1	2.584
5	8.453
10	10.457
15	11.004
20	10.275
25	10.157
30	8.835
35	6.822
40	3.087

* 3 replications, RSD ≤ 4%

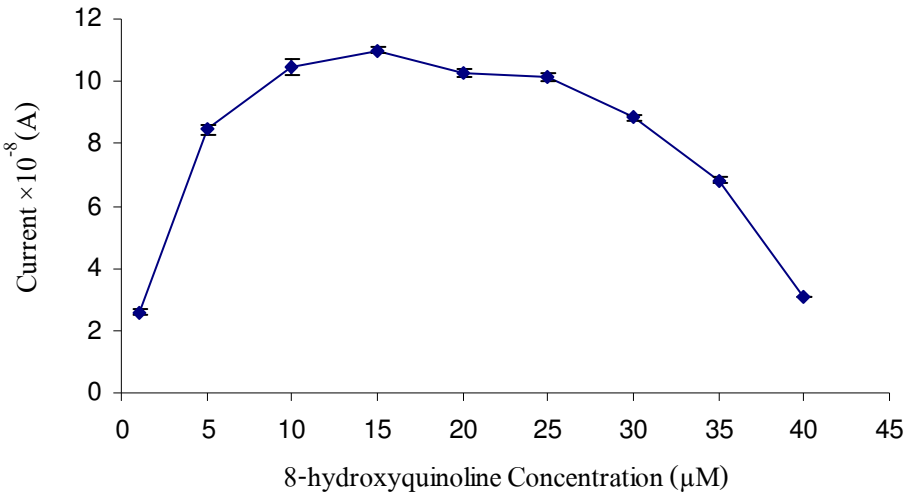

Figure 3-30 Effects of 8-hydroxyquinoline concentration on the peak current of 20 μg L^{-1} Pb(II) in 0.1 M ammonium acetate at pH = 7.5

The effect of 8-hydroxyquinoline concentration was shown that the stripping peak current for Pb(II) increased up to 15 M and in higher 8-hydroxyquinoline concentration the peak current heights decreased due to the competition of 8-hydroxyquinoline with Pb(II)-8-hydroxyquinoline complexes for adsorption onto the mercury drop electrode (Shemirani1 *et .al.,* 2005). Therefore, the 8-hydroxyquinoline concentration of 15 μM was selected as optimum value for further experiments.

3.4.8 Effect of accumulation potential

The effect of varying accumulation potential on the peak current for lead determination is shown in Table 3-17 and Figure 3-31. The accumulation potential was varied between -1.2 V and -0.2 V.

Table 3-17 Effects of accumulation potential on the peak current of 20 μg L^{-1} Pb(II) in 0.1 M ammonium acetate containing 15 μM 8-hydroxyquinoline at pH = 7.5

Potential (V)	Current $\times 10^{-8}$(A)
-1.2	10.477
-1.1	11.467
-1.0	11.695
-0.9	11.613
-0.8	11.771
-0.7	11.705
-0.6	11.692
-0.5	11.718
-0.4	11.521
-0.3	11.100
-0.2	10.709

* 3 replications, RSD $\leq$ 4%

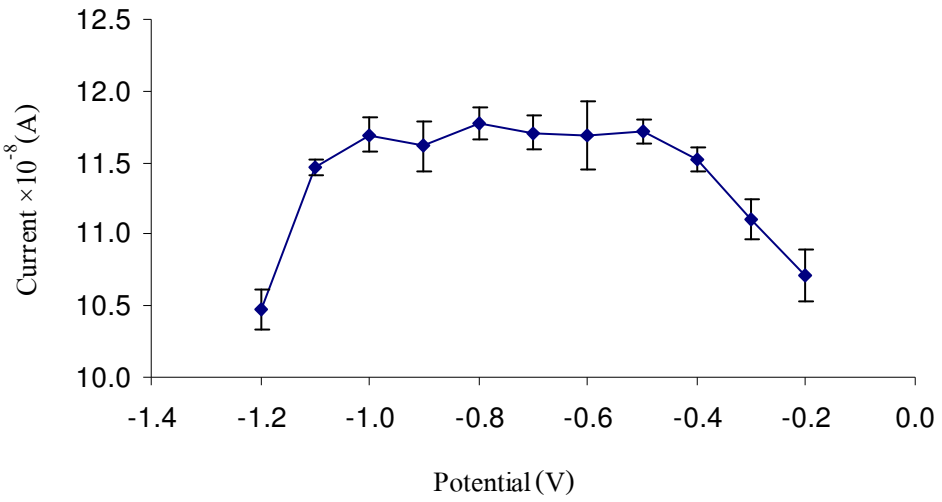

Figure 3-31 Effects of accumulation potential on the peak current of 20 µg L^{-1} Pb(II) in 0.1 M ammonium acetate containing 15 µM 8-hydroxyquinoline at pH = 7.5

It can be concluded from the results in Table 3-17 and Figure 3-31 that the peak current of Pb(II) was found constant between -0.8 V to -0.5 V. Thus, an accumulation potential of -0.7 V was selected for lead accumulation because the peak current at -0.7 V shown constant current and better sensitivity.

3.4.9 Effect of accumulation time

The effect of varying accumulation time on the peak current for Pb(II) determination is shown in Table 3-18 and Figure 3-32.

Table 3-18 Effects of accumulation time on the peak current of 20 μg L^{-1} Pb(II) in 0.1 M ammonium acetate containing 15 μM 8-hydroxyquinoline at pH = 7.5

Time (s)	Current $\times 10^{-8}$(A)
30	6.055
60	10.477
90	14.938
120	19.681
150	22.423
180	26.157
210	28.959
240	30.809
270	32.137
300	32.513
330	32.355
360	32.475

* 3 replications, RSD ≤ 3%

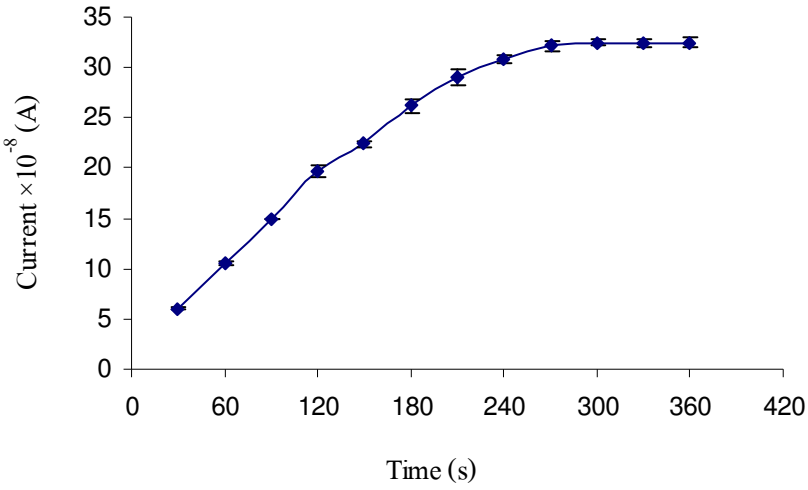

Figure 3-32 Effects of accumulation time on the peak current of 20 μg L^{-1} Pb(II) in 0.1 M ammonium acetate containing 15 μM 8-hydroxyquinoline at pH = 7.5

It can be concluded from the results in Table 3-18 and Figure 3-32 that the peak current of Pb(II) increased linearly with the accumulation time, gradually levelling off at periods longer than 270 s is presumably due to saturation of the HMDE surface at longer accumulation time (Amini and Kabiri, 2004). Thus, an adsorption time of 120 s was used throughout this work as it combines good sensitivity with relatively short analysis time.

3.4.10 Effect of scan rate and pulse amplitude

To improve the sensitivity for the determination of Pb(II), the influences of parameters of square wave voltammetry on the measurement of lead were studied. The effect of step potential and pulse amplitude on the peak current is shown in Table 3-19 – 3-20 and Figure 3-33 – 3-36

Table 3-19 Effects of scan rate on the peak current of 20 μg L^{-1} Pb(II) in 0.1 M ammonium acetate containing 15 μM 8-hydroxyquinoline at pH = 7.5

Scan rate (V/s)	Current $\times 10^{-8}$(A)
0.1	18.417
0.2	23.317
0.3	26.266
0.4	30.600
0.5	32.738
0.6	33.714
0.7	35.628
0.8	36.406
0.9	38.387

* 3 replications, RSD $\leq$ 5%

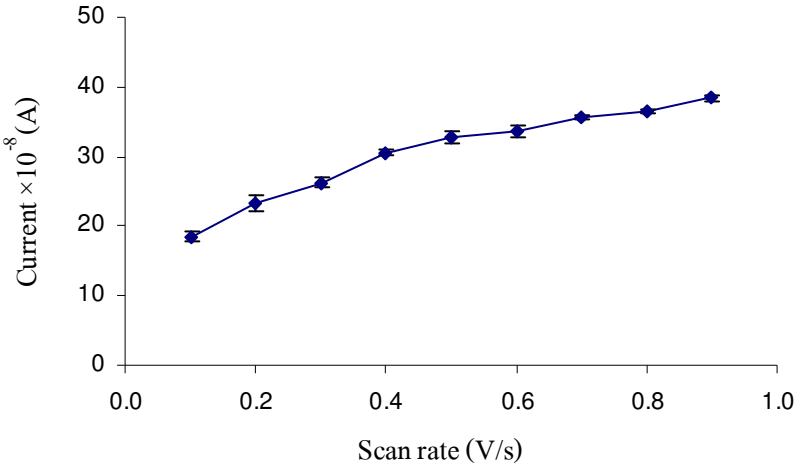

Figure 3-33 Effects of scan rate on the peak current of 20 µg L^{-1} Pb(II) in 0.1 M ammonium acetate containing 15 µM 8-hydroxyquinoline at pH = 7.5

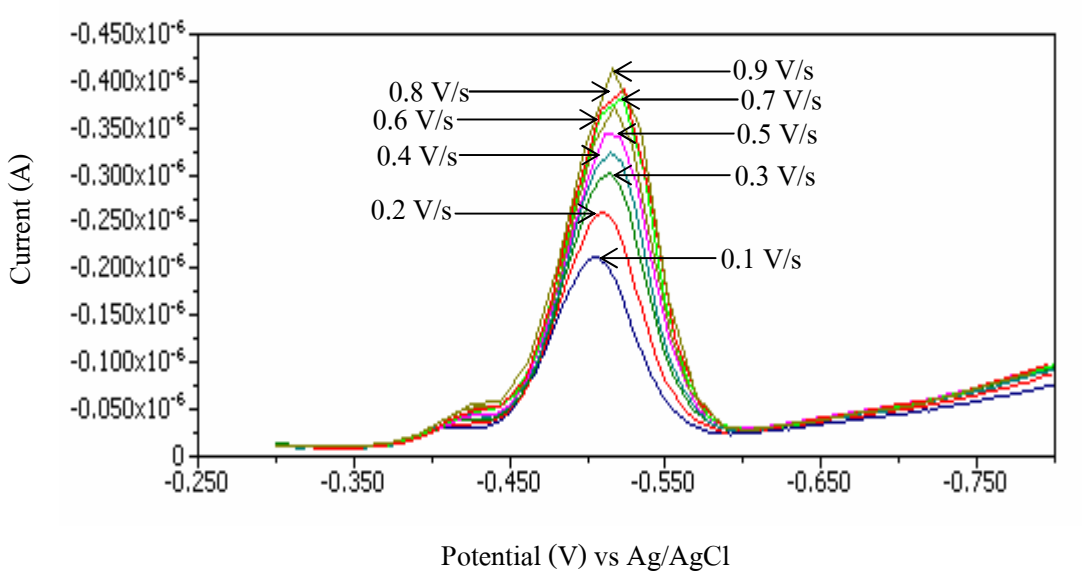

Figure 3-34 Voltammograms of varied scan rates on the peak current of 20 µg L^{-1} Pb(II) in 0.1 M ammonium acetate containing 15 µM 8-hydroxyquinoline at pH=7.5

Table 3-20 Effects of pulse amplitude on the peak current of 20 μg L^{-1} Pb(II) in 0.1 M ammonium acetate containing 15 μM 8-hydroxyquinoline at pH = 7.5

Pulse amplitude (mV)	Current $\times 10^{-8}$(A)
10	13.055
20	20.209
30	24.754
40	27.271
50	27.297

* 3 replications, RSD ≤ 2%

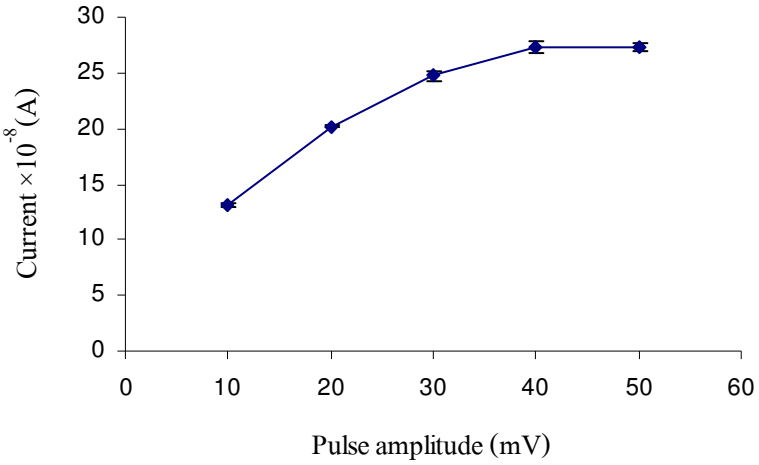

Figure 3-35 Effects of pulse amplitude on the peak current of 20 μg L^{-1} Pb(II) in 0.1 M ammonium acetate containing 15 μM 8-hydroxyquinoline at pH = 7.5

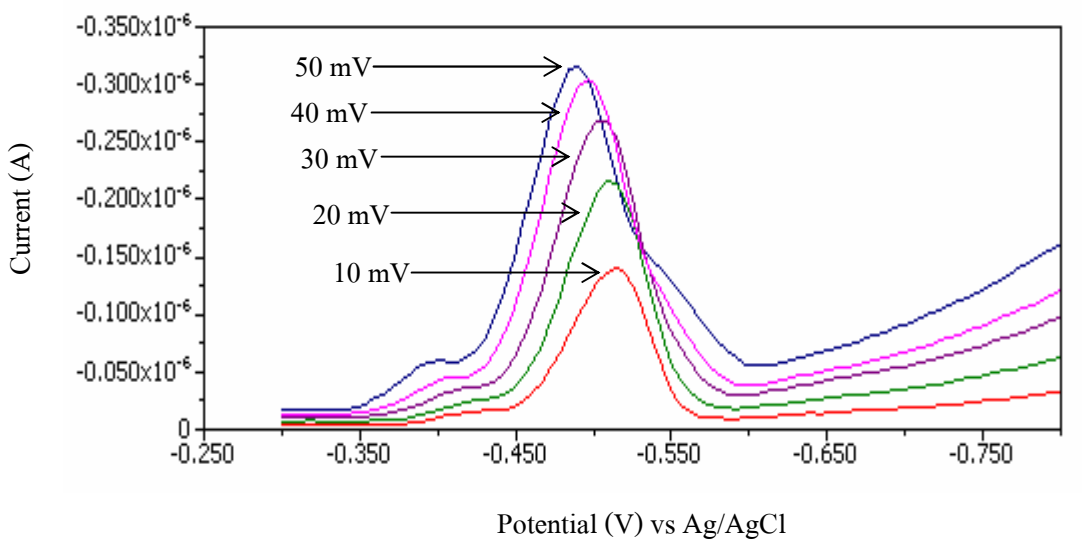

Figure 3-36 Voltammograms of varied pulse amplitude on the peak current of 20 µg L^{-1} Pb(II) in 0.1 M ammonium acetate containing 15 µM 8-hydroxyquinoline at pH = 7.5

The dependence of peak currents on the scan rate step potential and pulse amplitude under the optimal conditions was also investigated in the range of 0.1 – 0.9 V s^{-1} and 10 - 50 mV. The peak current for lead increased with increasing scan rate and pulse amplitude. Therefore, a scan rate of 0.3 V s^{-1} and pulse amplitude 20 mV were selected because of the better sensitivity and peak shape.

3.5 Analytical performances

3.5.1 Linear range

The linear range is defined as the concentration range over which the intensity of the signal obtained is directly proportional to the concentration of the analyte producing the signal (IUPAC, 1997). The linear range is determined by plotting the peak current of the signal versus the concentration of lead standard solution. It is desirable to work within the linear region of the resulting calibration curve.

The calibration graph of Pb(II) at various concentrations is shown in Table 3-21 and Figure 3-37. It was found that the linear dynamic range of Pb(II) was from 0.5 - 90.0 μg L^{-1} with correlation coefficient 0.9973.

Table 3-21 The current of Pb(II) at the different concentration

Pb(II) concentration (μg L^{-1})	Current $\times 10^{-8}$(A)
0.5	0.893
1	1.645
5	5.778
10	13.911
20	27.021
30	37.718
40	48.356
50	61.682
60	74.014
70	82.528
80	91.795
90	103.049
100	104.339
110	107.045
120	112.882

*3 replications, RSD $\leq$ 6%

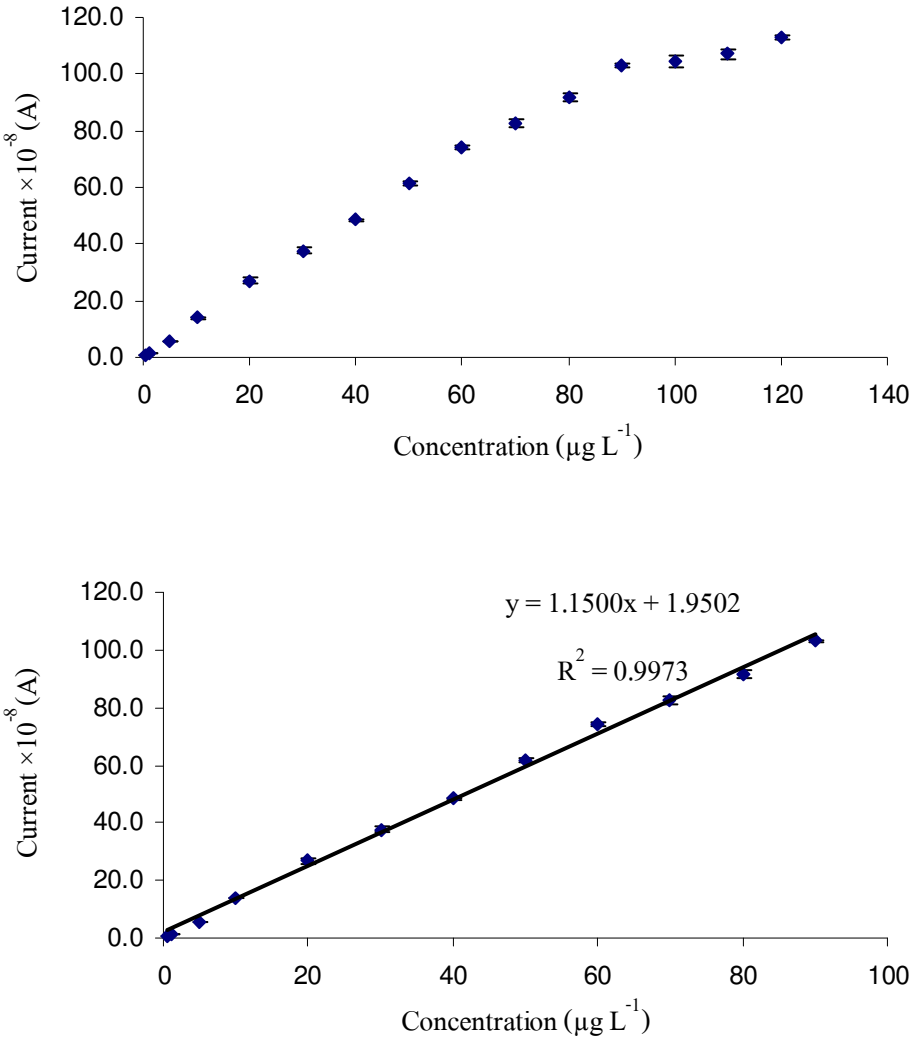

Figure 3-37 The calibration graph of Pb(II) at the different concentration; (a) 0.5 -120.0 µg L^{-1}, (b) 0.5-90.0 µg L^{-1}

3.5.2 The limit of detection (LOD) and the limit of quantification (LOQ)

The limit of detection (LOD) and the limit of quantification (LOQ) of Pb(II) was studied by measuring the peak current of ten replications of the blank. The limit of detection and the limit of quantification were calculated from the equation in section 2.4.2. The equation is shown as follows.

The limit of detection = (3*SD)/*m*

The limit of quantification = (10*SD)/*m*

When, SD = standard deviation of blank

m = slope of calibration graph

Table 3-22 The peak current of Pb(II) in reagent blank (n = 10)

Replicate	Current × 10^{-8}(A)
1	0.246
2	0.256
3	0.128
4	0.176
5	0.219
6	0.276
7	0.274
8	0.204
9	0.182
10	0.224
Mean	0.218
SD	0.047
Calib. Slope	1.3131
LOD	0.108
LOQ	0.360

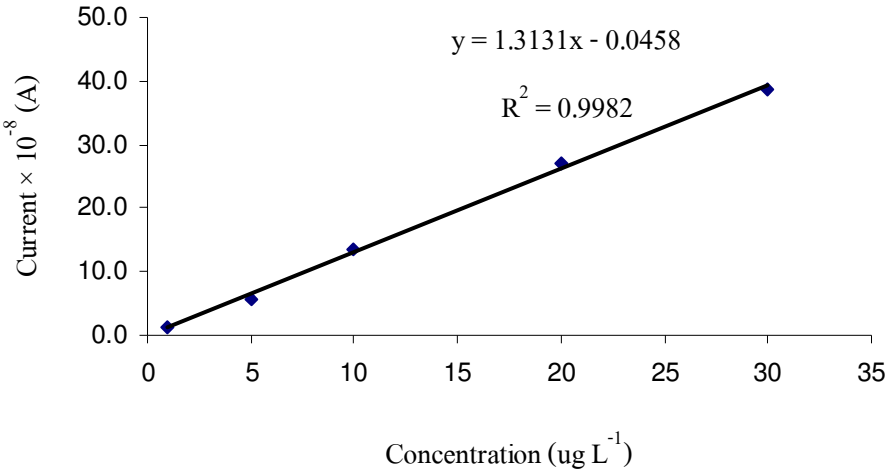

Figure 3-38 The calibration curve of Pb(II)

The peak current of blank was carried out for evaluating the limit of detection and the limit of quantification of Pb(II). The results are shown in Table 3-22 and Figure 3-38. The limit of detection of Pb(II) is 0.108 µg L^{-1} and the limit of quantification of Pb(II) is 0.360 µg L^{-1}.

3.5.3 Accuracy and precision

Accuracy

The accuracy of the concentrations determined in this study was checked by spiking the canned fish samples before sample digestion with various concentration of Pb(II) for the percent recovery. The result is shown in Table 3-23. The percent recovery values were obtained in the range 93.68 - 95.13%.

Table 3-23 The percent recovery of Pb(II) at concentration of 10, 20 and 30 µg L^{-1} in canned fish

Experment	Pb(II) concentration (µg L^{-1})	%Recovery
sample	9.582	-
sample + 10 ug/L	18.984	94.02
sample + 20 ug/L	28.318	93.68
sample + 30 ug/L	38.121	95.13

Precision

The precision of the adsorptive cathodic stripping voltammetry method was also evaluated as %RSD of ten replication measurement. The %RSD of 1.0, 5.0 and 10.0 μg L^{-1} Pb(II) was obtained from this method were 6.23%, 2.40% and 2.00% respectively. The result is shown in Table 3-24.

Table 3-24 The current of Pb(II) for evaluating the precision

Replicate	Current $\times 10^{-8}$ (A)		
	1 μg L^{-1} Pb(II)	5 μg L^{-1} Pb(II)	10 μg L^{-1} Pb(II)
1	1.501	6.429	13.023
2	1.533	6.864	13.821
3	1.573	6.689	13.461
4	1.533	6.643	13.062
5	1.622	6.530	13.234
6	1.688	6.633	13.620
7	1.688	6.684	13.528
8	1.714	6.473	13.174
9	1.714	6.337	13.553
10	1.816	6.444	13.601
average	1.638	6.572	13.408
SD	0.102	0.158	0.267
%RSD	6.23	2.40	2.00

3.6 The comparision of the calibration and standard addition method for determination of Pb(II) in canned fish samples

This experiment was performed to compare standard method between calibration and standard addition for determination of Pb(II) in canned fish samples by AdCSV method. The results are shown in Table 3-25 and Figure 3-39.

Table 3-25 The comparison of current using calibration and standard addition method for Pb(II) determination in canned fish samples

Pb(II) Concentration ($\mu g\ L^{-1}$)	Current $\times 10^{-8}$(A)	
	Calibration	Standard addition
0	0.000	0.379
2	3.365	2.424
4	7.561	5.124
6	11.612	7.621

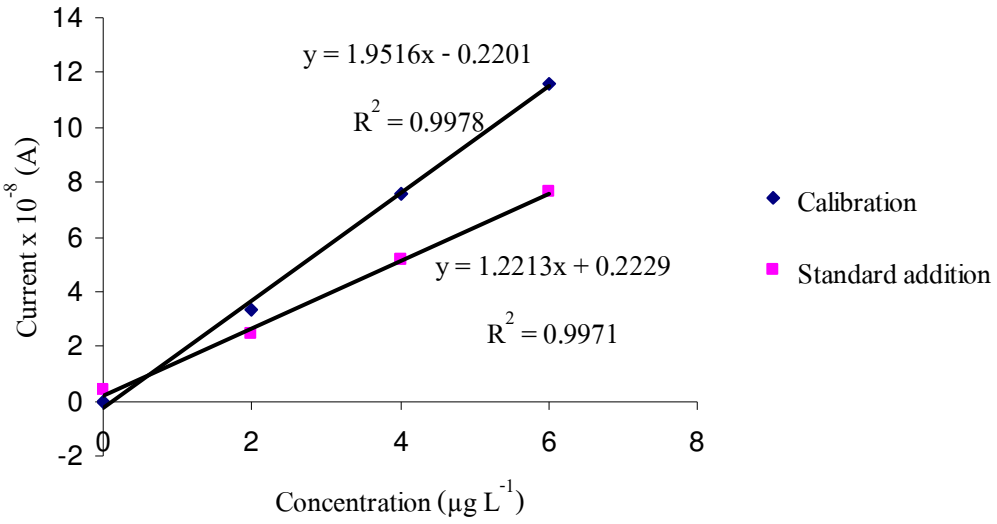

Figure 3-39 The comparison of current using calibration and standard addition method for Pb(II) determination in canned fish sample

The slope of the calibration and the standard addition were compared using two-way ANOVA. In making a significance test, a true of hypothesis which is known as a null hypothesis, denote by H_0 that the interaction of both slope is not significant and alternative hypothesis (H_1) that the interaction of both slope is significant. If *P* value is less than α (level of significance) then the null hypothesis was rejected at that significant level.

Table 3-26 Result of statistical test using two-way ANOVA by R software

Matrix	*Df*	Sum Sq	Mean Sq	*F*	P
Canned fish	3	16.020	5.340	178.71	$1.639\times10^{-12***}$

Significant codes: '***' 0.001

Where: *Df* is the degree of freedom (*Df* = n-1, n is the number of concentration)

Sum Sq is the sum of squares, it refers toan interim quantity used in the calculation of an estimate of the population variance

Mean Sq is mean square, it refer to a sum of squared terms divided by the number of degrees of freedom

F is the ratio of two sample variances

P is probability

From the results in Table 3-26 it can be concluded that the slope of regression line in the calibration curve and the standard addition curve of method was significant difference ($P < 0.001$). Accordingly, it can be concluded that the matrix effect can affect the analysis. Therefore the standard addition was the suitable method for Pb(II) determination in canned fish samples.

3.7 Interference studies

Possible interference by other metals with the cathodic adsorptive stripping voltammetry determination of Pb(II) was investigated by the addition of the interfering ion to a solution containing 20.0 μg L^{-1} of Pb(II) and carrying out the measurements at the optimized conditions. The results of this study are summarized in Table 3-27.

Table 3-27 Change in peak current of 20 μg L^{-1} Pb(II) in the presence of other ions

Metal Interferences	Concentration (μg L^{-1})	Change in peak current (%)
Fe^{2+}	100	-0.3
Mn^{2+}	100	7.7
Cr^{3+}	100	4.3
Hg^{2+}	100	-1.4
Sn^{2+}	60	-10.8
Cd^{2+}	20	-13.7
Zn^{2+}	20	-8.2
Al^{3+}	20	-12.9
Cu^{2+}	20	-32.9
Ni^{2+}	20	-29.5

From the result, it can be concluded that several ions such as Fe^{2+}, Cr^{3+}, Mn^{2+} and Hg^{2+} (5-fold concentration); Sn^{2+} (3-fold concentration); Cd^{2+}, Zn^{2+}, and Al^{3+} (equal concentration); have only negligible effect on the determination Pb^{2+}. However, equal concentration amount of Cu^{2+} and Ni^{2+} interfere significantly by decreasing the Pb^{2+} signal, but the peak of Pb^{2+} is still well separated from all of them.

3.8 Determination of Pb(II) in canned fish samples

The proposed method was applied to the determination of Pb(II) in canned fish samples from Lotus supermarket. The samples were digested by hot plated digestion method (2.5). The standard addition method was used, in order to eliminate the matrix effect. The results are shown in Table 3-28.

Table 3-28 The Pb(II) concentration in canned fish samples by standard addition method

Sample no.	Pb Concentration (μg g^{-1}) (wet weight)
1	0.160
2	0.285
3	0.208
4	0.180
5	0.259
6	0.151
7	0.140
8	0.265
9	0.121
10	0.277

*3 replications, RSD $\leq$ 15%

The concentrations of Pb(II) in canned fish samples (wet weight) were found in range 0.121 – 0.285 μg g^{-1}. However, the concentration of Pb(II) in canned fish samples were lower than the food contamination standard limited level. The standard concentration of Pb(II) issued by the Ministry of Public Health of Thailand is less than 1.00 μg g^{-1}.